Nanocrystalline zirconia based powders synthesized by hydrothermal method[#]

Viktoria Tsukrenko[*], Elena Dudnik, Alexey Shevchenko

Frantsevich Institute for Problems of Materials Science of National Academy of Sciences of Ukraine, 3, Krzhyzhanovsky Str., Kyiv 03142, Ukraine

Abstract

Nanocrystalline powders in the ZrO_2-Y_2O_3-CeO_2-CoO-Al_2O_3 system with 1 and 10 mol% Al_2O_3 were prepared via hydrothermal treatment in alkaline medium. The characteristics of nanocrystalline powders after heat treatment in the temperature range from 500 to 1200 °C were investigated by XRD phase analysis, scanning electron microscopy, petrography and BET measurements. It was found that hydrothermally treated powders contained metastable low-temperature cubic solid solution based on ZrO_2 and addition of Al_2O_3 increased temperature of phase transformation of the metastable cubic- ZrO_2 to tetragonal-ZrO_2. It was evidenced that both powders remained nanocrystalline after all processing steps with the average particle sizes from 8 to 20 nm. The addition of 0.3 mol% CoO allows one to obtain composites with good sinterability at 1200 °C

Keywords: zirconia, nanocrystalline powder, hydrothermal treatment

I. Introduction

Zirconia-based composites incorporate high strength, fracture toughness, corrosion resistance, low thermal conductivity, refractoriness, ionic conduction and bioinertness. The high fracture behaviour of these ceramics resulted from the martensitic phase transformation of tetragonal zirconia (T-ZrO_2) into monocline zironia (M-ZrO_2) [1]. Nowadays a variety of composites based on binary and ternary ZrO_2 systems have been developed [2]. For example, ZrO_2-Y_2O_3 and ZrO_2-Al_2O_3 composites have high strength and ZrO_2-CeO_2 composites high fracture toughness. Ceramics based on ternary systems may possess higher strength (ZrO_2-Y_2O_3-Al_2O_3) or higher strength and fracture toughness (ZrO_2-Y_2O_3-CeO_2) then the binary materials. Zirconia-based materials that are the most appropriate for producing of bioimplants, engineering ceramics and solid electrolytes for low-temperature fuel cells are based on various multiphase composites. They are de-signed under the subsolidus range and mainly represent composites consisting of ZrO_2-based solid solutions (T-ZrO_2) and fine α-Al_2O_3 particles. The properties of composites in the system ZrO_2-Y_2O_3-CeO_2-Al_2O_3 depend on the properties of materials based on the bounding binary and ternary systems. Hence, composites with different microstructures and toughening mechanisms may be developed in this system [3].

Implants based on ZrO_2 have been developed as an alternative to implants based on Al_2O_3. One of the reasons for using ZrO_2 in orthopedics is its fracture behaviour resulted from transformation toughening [4,5]. Designing the bioinert implant, possessing the enhanced phase stability in living organism, is one of the directions to develop composites in the ZrO_2-Y_2O_3-CeO_2-Al_2O_3 system. For enhancing the contrast of implants against living tissue, cobalt oxide was introduced to colour the composite [6,7].

The application of complex physicochemical techniques, mechanical and thermal treatments at the very first stages of nanocrystalline powders production is a necessary for the structure and properties control of a created material. So far there is no universal process for producing nanocrystalline powders that would ful-

---

[#] Paper presented at *Conference for Young Scientists - 9th Students' Meeting, SM-2011,* Novi Sad, Serbia, 2011
[*] Corresponding author: tel: *+380 44 424 3573*
fax: *+380 44 424 2131, e-mail: tsukrenko@ipms.kiev.ua*

ly comply with production requirements for any class of ceramics. In general, there is a need for nanocrystalline powders with complex chemical composition, narrow particle size distribution, high purity and homogeneity, and sintering activity to produce such ZrO_2-based ceramics. For their production wet chemical methods are primarily used: coprecipitation, cryochemical, sol-gel methods, hydrolysis of metal alcoholates and hydrothermal synthesis [8–14]. We believe that the most appropriate method for producing qualitative and effective ZrO_2-based powders in the ZrO_2-Y_2O_3-CeO_2-Al_2O_3-CoO system is hydrothermal treatment of a coprecipitated hydroxide mixture. The choice of an alkaline medium to produce nanocrystalline powders with complex composition in this system is governed by the chemical properties of oxide components [3,15].

The purpose of this work was to investigate characteristics of two nanocrystalline powders with different compositions: $95.2ZrO_2$-$2.8Y_2O_3$-$0.7CeO_2$-$0.3CoO$-lAl_2O_3 and $86.2\%ZrO_2$-$2.8\%Y_2O_3$-$0.7\%CeO_2$-$0.3\%CoO$-$10\%Al_2O_3$, prepared under hydrothermal conditions. The powder compositions were selected in existence region of the T-ZrO_2, limiting to the ZrO_2-Y_2O_3-CeO_2-CoO-Al_2O_3 system. The characteristics of the nanocrystalline powders were studied after their heat treatment in the temperature range from 500 to 1200 °C.

II. Experimental

Two different zirconia-based powders with following compositions (mol%) $95.2ZrO_2$-$2.8Y_2O_3$-$0.7CeO_2$-$0.3CoO$-lAl_2O_3 (sample with notation Al) and $86.2\%ZrO_2$-$2.8\%Y_2O_3$-$0.7\%CeO_2$-$0.3\%CoO$-$10\%Al_2O_3$ (sample with notation A10) were synthesized from reagent-grade chemicals: zirconyl nitrate ($ZrO(NO_3)_2 \times 2H_2O$), yttrium nitrate ($Y(NO_3)_3 \times 6H_2O$), cerium nitrate ($Ce(NO_3)_3 \times 6H_2O$), aluminum nitrate ($Al(NO_3)_3 \times 9H_2O$), and cobalt nitrate ($Co(NO_3)_3 \times 2H_2O$). Hydroxides were obtained through homogeneous coprecipitation from an appropriate mixture of aqueous solutions of the starting salts, using aqueous NH_4OH as the precipitant. After heating at 35 °C with constant stirring, the reaction system was boiled for 3–4 h. As a result, we obtained dull, translucent gel-like substances, consisting of zirconium, yttrium, cerium, aluminum and cobalt hydroxides. The obtained hydroxide mixtures were washed many times with distilled water by decantation. Distilled water in the ratio 1 : 2 was added to the gel-like substances for the hydrothermal treatment. The treatment was performed in a laboratory autoclave at 210 °C for 3 h. Dehydration under the hydrothermal conditions led to the formation of a well-defined interface between the mother liquor and the suspended precipitate. The separated precipitates were washed many times with distilled water, collected on a vacuum filter and dried at 90–95°C for 8 h. To study the effect of heat treatment on the structure and phase composition of the resultant nanocrystalline powders, the dried samples were heat treated at 500, 700, 900 and 1200 °C for 1.5 h at each temperature.

Characterization of the heat treated nanocrystalline powders were determined by X-ray diffraction (XRD), scanning electron microscopy (SEM), petrography and low-temperature nitrogen adsorbtion (BET). XRD characterisation was performed with a DRON-1.5 powder diffractometer ($Cu_{K\alpha}$ radiation, Ni filter). The scan rate varied from 1 to 4 °/min. The average crystallite size was determined using the Scherrer formula: $D = 0.89 \cdot \lambda / (\beta \cdot \cos\theta)$, where λ is X-ray wavelength, β is full-width at half height of an observed peak and θ is the diffraction angle. Microscopic examination was carried out on a scanning electron microscope CAMEBAX SX-50 with the backscattered electrons (COMPO and BSE) and secondary reflected electrons (SE). For microstructural and phase analyses we used MIN-8 optical microscope (magnification from 60× to 620×) and a standard set of immersion media. The specific surface area of the nanocrystalline powders after different processing steps was determined by low-temperature adsorption of nitrogen in the flow of nitrogen/helium mixture on MPP 2 unit (Sumperk, Slovakia).

III. Results

3.1 Powders after hydrothermal treatment

After hydrothermal treatment both powders contained metastable low-temperature, cubic solid solution based on ZrO_2 (F-ZrO_2) (Fig. 1). The formation of the metastable F-ZrO_2 during hydrothermal treatment can be accounted for a number of factors. The polymeric zirconium hydroxycomplex, forming during hydrothermal treatment, $[Zr(OH)_2 \cdot 4H_2O]^{8+}_4$, is close to the cubic ZrO_2 structure [15]. Consequently, the formation of the metastable F-ZrO_2 is consistent with the Dankov principle [16]. Moreover, the size factor is also of importance. The crystallite sizes of F-ZrO_2 are about 8 nm in both powders. The particles in the Al and A10 powders formed "soft" rounded agglomerates with the dominant sizes 5–10 μm and 3–5 μm, respectively (Fig. 2.a,f).

Petrography enhanced capabilities of the powders phase composition investigations. A microstructural analysis showed that the two-phase agglomerates are present in both powders. The first phase is the colourless isotropic phase with $1.710 < n < 1.714$ (refraction index of ZrO_2 is 2.04). In agglomerates of the powder A1 rounded fine grains were observed (as the second phase) in the isotropic phase. The grains refraction index is larger then the refraction index of the colourless isotropic phase. In agglomerates of the powder A10 the plate-like fine grains were observed in the isotropic phase. The plate's refraction index is below the refraction index of the colourless isotropic phase. Concern-

ing crystal optical characteristics, there are isotropic F-ZrO_2 and γ-Al_2O_3 as well as anisotropic T-ZrO_2, M-ZrO_2, boehmite, and δ-, θ-, α-Al_2O_3.

Thus, X-ray amorphous precipitate was formed after coprecipitation and crystallisation occurred in precipitate under the hydrothermal treatment, but part of the precipitate remained amorphous. The amorphous colourless isotropic phase of the precipitate was identifies as the enclosing phase. Most probably, the F-ZrO_2 grains were crystallized in rounded form in the powder

A1, whereas the boehmite grains were crystallized in plate-like form in the powder A10. The powders isotropy after hydrothermal treatment was conditioned by their nanocrystallinity.

Figure 3 shows, that the specific surface area of the A10 powder is twice as much as of the Al powder after hydrothermal treatment. The apparent reason for this is that the agglomerates differ in porosity. According to the microstructural analysis the porosity in the A10 powder exceeded it in the Al powder.
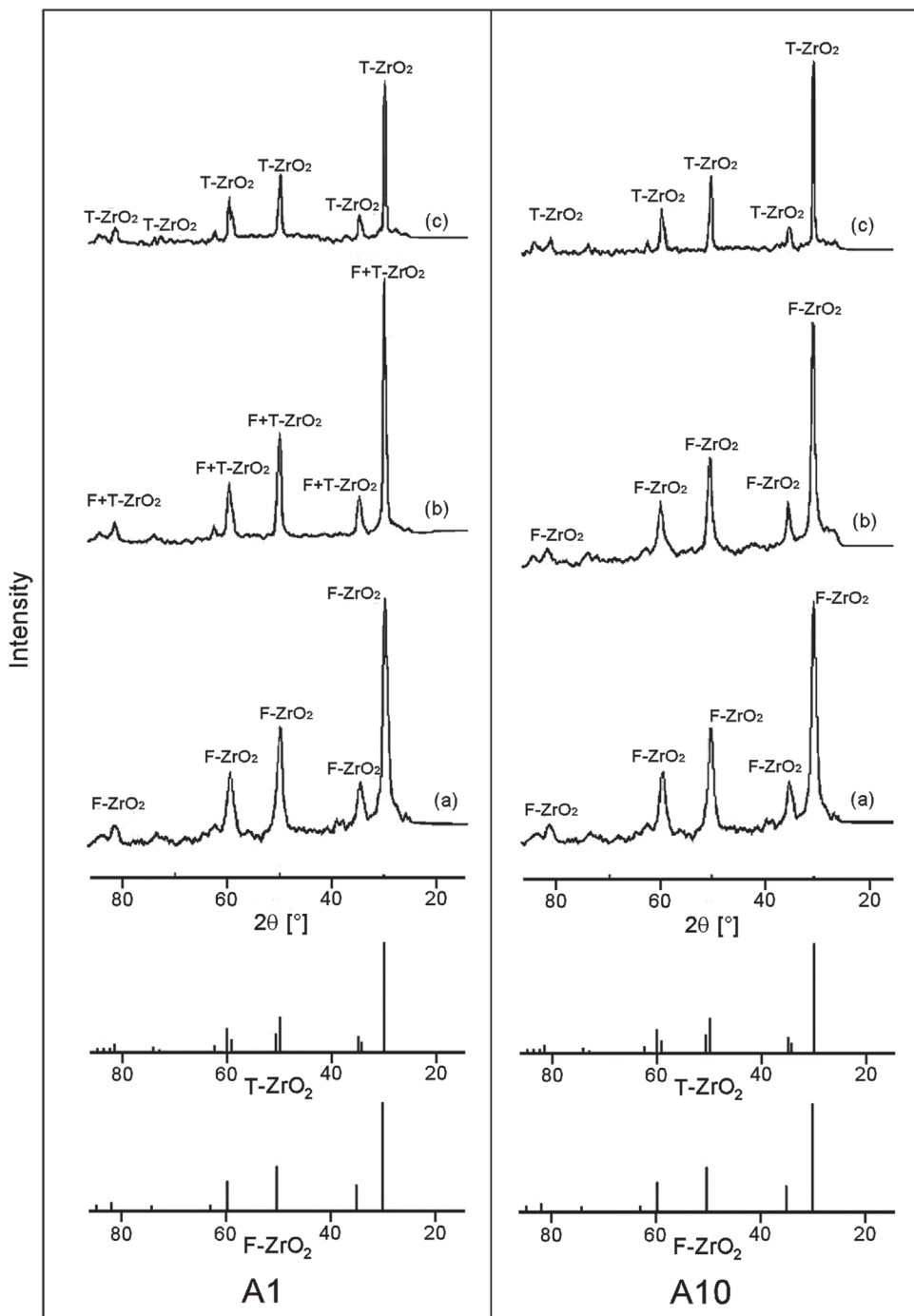
Figure 1. XRD patterns of A1 and A10 nanocrystalline powders after hydrothermal treatment at 210 °C (a) and heat treatment at temperature 900 °C (b) and 1200 °C (c)

153

3.2 Powders heated at 500 °C

According to XRD results, heat treatment at 500 °C had no effect on the phase composition of the powders. The primary particles sizes were constant, however, at the same time, the specific surface area of powders increased almost twice (Fig. 3). These changes can be explained by the removal of the adsorbed and hydration water from the multicomponent hydrothermal powders during heat treatment below 500 °C. As it was shown earlier [18], these processes occur in the temperature ranges 60–120 °C and 320–500 °C depending on composition. They led to loosening of agglomerates and increasing their porosity. The size of the A1 powder agglomerates was not changed whereas the average size of the A10 agglomerates increased to 10 μm (Fig. 2b,g). A microstructural analysis showed that the colourless isotropic phase remained in both powders at 500°C (but had higher refractive index) and a fine-grained mixture of the anisotropic and isotropic phases showed up with the size beyond the resolving power of an optical microscope. The amount of the isotropic agglomerates, milky in polarized light, has increased. It is reasonable to assume that heat treatment at 500 °C initiates a low-temperature $F\text{-}ZrO_2 \rightarrow T\text{-}ZrO_2$ phase transformation, which can be identified only from crystal-optical characteristics.

3.3 Powders heated at 700 °C

When temperature increased to 700 °C the refractive index of the colourless isotropic phase increased (n £ 2.04) and the content of the fine-crystalline mixture of anisotropic and isotropic phases became higher. This is evidence of the phase transition $F\text{-}ZrO_2 \rightarrow T\text{-}ZrO_2$. Primary particles sizes of both powders were the same. After heat treatment at 700 °C the specific surface area of the A1 powder was decreased monotonically, whereas the one of the A10 powder dropped nonlinearly (Fig. 3). These processes were accompanied by phase transformations of the low-temperature forms of Al_2O_3 [19], Co_3O_4 formation [20] and sintering of powders. Individual transparent isotropic regions with a refraction index » 2.04 were found in the A10 powder. Apparently, there are sintered agglomerates consisting of ZrO_2 nanocrystalline particles. As seen in Fig. 2c,h the average agglomerate size were reduced by half.

3.4 Powders heated at 900 °C

Over 900 °C $F\text{-}ZrO_2$ retained in the A10 powder, whereas in the A1 powder both F- and $T\text{-}ZrO_2$ were found by XRD. It was confirmed that the $F\text{-}ZrO_2 \circledR T\text{-}ZrO_2$ transformation process occurred (Fig. 1). The primary particle size was not varied in both powders. $F\text{-}ZrO_2$ remained in the powder A10 due to the effect of mutual influence on grain growth in hydrothermal ZrO_2 based powders containing Al_2O_3 [22]. Investigations of nanocrystalline hydrothermal powders with various compositions showed that low-temperature modifica-

tions of Al_2O_3 appear consistently during heat treatment and a-Al_2O_3 can be formed at 850 °C [18,19]. The reflections from low-temperature Al_2O_3 polymorphs were not found in the XRD-patterns (Fig. 1), apparently, due to low content of these polymorphs in the A1 and A10 powders.

Morphology of the powders heat treated at 900 °C is similar to that obtained after heat treatment at 700 °C (Fig. 2d,i). The densification of the agglomerates continues, the area of contacts between them further increases, and the average size of the agglomerates reaches 20 and 40 μm in the A10 and A1 powders, respectively.

The specific surface area of the A1 powder drops sharply, whereas decreasing of the A10 powder specific surface area becomes slower (Fig. 3). This is related to the complex nature of the processes that take place in both nanocrystalline Al and A10 powders. Microstructural investigation had shown that the morphology of the A1 powder was varied topologically continuous. In contrast, dense sintered fine-grained agglomerates with size from 10 to 40 μm appeared in the A10 powder. Sintered agglomerates are characterized by milky polarization. The ZrO_2 phase transformations and sintering processes are accompanied by the formation of $\alpha\text{-}Al_2O_3$ [19] and CoO [20]. Both powders were white in colour after hydrothermal treatment and heating at 500, 700 and 900 °C.

3.5 Powders heated at 1200 °C

According to XRD results (Fig. 1), heat treatment at 1200 °C resulted in the finish of phase transformation of the metastable $F\text{-} ZrO_2$ to $T\text{-}ZrO_2$ in both powders. The A1 powder turned more bright blue, than A10, that indicates the formation of cobalt aluminate spinel, $CoAl_2O_4$ [21]. The $CoAl_2O_4$ formation is accompanied by a twofold increase in ZrO_2 crystallite size and a sharp decrease in the specific surface area of the powders (Fig. 3). It should be noted that, for hydrothermal nanocrystalline ZrO_2 based powders in the $ZrO_2\text{-}Y_2O_3\text{-}CeO_2\text{-}Al_2O_3$ system, the similar decreasing of specific surface area was observed at higher temperature, i.e. 1300 °C [3,18,19,22]. Thus, it can be assumed that with addition of CoO the sintering temperature of ZrO_2-based nanocrystalline powders is reduced to 1200 °C in the $ZrO_2\text{-}Y_2O_3\text{-}CeO_2\text{-}Al_2O_3$ system. Primary particles sizes in both powders are 20 nm and the sintering of both powders is accelerated. Figures 2e,j shows the formation of a sintered skeletal structure of agglomerates.

Microstructural investigations showed that the opaque vitrified agglomerates were formed in both powders. Agglomerates with size up to 8–40 μm are rounded. Single grains of $T\text{-}ZrO_2$, up to 1 μm, are present in the A1 powder. Single sintered agglomerates about 20 μm were found in A10 powder and consisted of $T\text{-}ZrO_2$ fine grains.
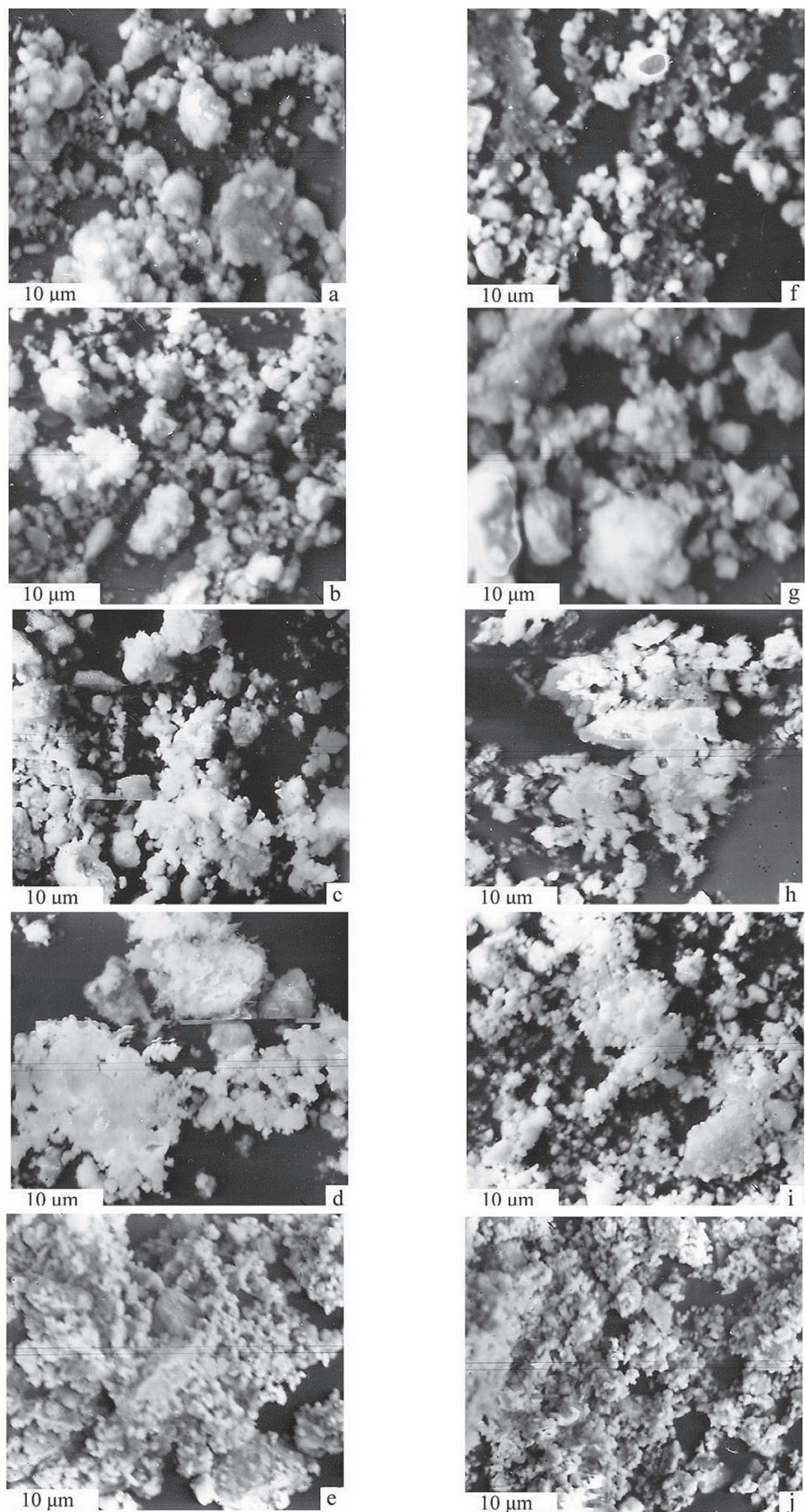
Figure 2. SEM images showing the nanocrystalline powders A1 (a-e) and A10 (f-j): after hydrothermal treatment (a,f) and heat treatment at 500 °C (b,g), 700 °C(c,h), 900 °C(d, i) and 1200 °C (e,j)
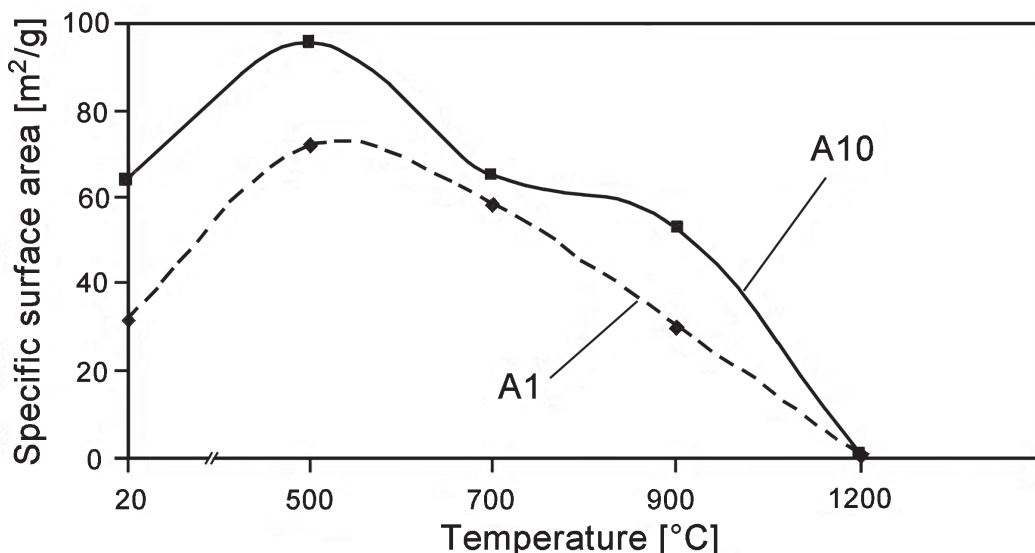
Figure 3. Effect of heat treatment on the specific surface area of the nanocrystalline ZrO2-Y2O3-CeO2-CoO-Al2O3 powders

IV. Discussion

The nanocrystalline multicomponent powders in the ZrO_2-Y_2O_3-CeO_2-Al_2O_3-CoO system are nonequilibrium thermodynamic systems with a high surface free energy, which retain their reactivity during heat treatments at 500, 700, 900 and 1200 °C. This is evidenced by the fact that the A1 and A10 powders remained nanocrystalline after all processing steps.

We identified a number of general trends in the variation of the Al and A10 powders characteristics during heat treatment. In particular, the formation of metastable F-ZrO_2 and the F-ZrO_2→T-ZrO_2 low-temperature phase transition occur sequentially in identical temperature ranges. However, the temperature of the phase transformation in the A1 powders was lower then in the A10 powder. It is attributed to the mutual inhibition effect of zirconia and alumina crystallisation that is typical for hydrothermal nanocrystalline powders.

The variation in the morphology of the powders is topologically continuous. At temperatures below 900 °C, the sintering process does not involve active growth of the ZrO_2 crystallites. Above this temperature, the phase transformations of alumina and cobalt oxide accelerate the growth of the ZrO_2 crystallites. In the range 700–900 °C the ZrO_2 and Al_2O_3 particles probably inhibited the growth of each other [22]. After heat treatment at 1200 °C, both powders were bright blue in colour, which was due to the formation of cobalt aluminate spinel $CoAl_2O_4$. The spinel reduced the mutual inhibition of structural changes and caused a twofold increase in ZrO_2 crystallite size up to 20 nm. In these powders a "skeletal" microstructure forms at 100 °C lower than in nanocrystalline ZrO_2-Y_2O_3-CeO_2-Al_2O_3 powders [3,18,19,22]. This indicates that the prepared powders retain sinterability at a reduced temperature (1200 °C)

and that one can produce composites sufficiently stable to aging because no M-ZrO_2 was found in the powders.

V. Conclusions

The characteristics of nanocrystalline powders with the compositions (mol%) 95.2ZrO_2-2.8Y_2O_3-0.7CeO_2-0.3CoO-lAl_2O_3 and 86.2%ZrO_2-2.8%Y_2O_3-0,7%CeO_2-0.3%CoO-10%Al_2O_3 produced by hydrothermal treatment in alkaline medium were investigated. It was found that under hydrothermal conditions in these powders the low-temperature metastable F-ZrO_2 was formed. During the thermal treatment of powders in the temperature range 500–1200 °C phase transformations of ZrO_2 as well as alumina and the formation of CoA-l$_2O_4$ occurred. The temperature of phase transformation F-ZrO_2→T-ZrO_2 increases from 900 to 1200 °C with increasing the Al_2O_3 content in the powders from 1 to 10 mol%. Varying of the powders morphology is topologically continuous. The $CoAl_2O_4$ formation reduces the powders sintering temperature for 100 °C.

References

1. R.H.J. Hannink, P.M. Kelly, B.C. Muddle, "Transformation toughening in zirconia-containing ceramics", *J. Am. Ceram. Soc.*, **83** [3] (2000) 461–487.
2. A.V. Shevchenko, A.K. Ruban, E.V. Dudnik, "High-technology ceramics based on zirconia", *Refractor. Technic. Ceram.*, **9** (2000) 2–8.
3. E.V. Dudnik, A.V. Shevchenko, A.K. Ruban, V.P. Red'ko, L.M. Lopato, "Microstructural design of ZrO_2-Y_2O_3-CeO_2-Al_2O_3 materials", *Powder Metall. Metal Ceram.*, **49** [9-10] (2011) 528–536.

4. J. Chevalier, "What future for zirconia as a biomaterial?", *Biomaterials,* **27** (2006) 535–543.

5. P.F. Manicone, R.P. Iommetti, L. Raffaelli, "An overview of zirconia ceramics: Basic properties and clinical applications", *J. Dentistry*, **35** (2007) 819–826.

6. N. Ouahdi, S. Guillemet, J.J. Demai, B. Durand, L. Er Rakho, R. Moussa, A. Samdi, "Investigation of the reactivity of AlCl$_3$ and CoCl$_2$ toward molten alkali-metal nitrates in order to synthesize CoAl$_2$O$_4$", *Mafcna/s Lett.,* **59** (2005) 334–340.

7. E.V. Dudnik, V.V. Tsukrenko, A.V. Shevchenko, A.K. Ruban, L.M. Lopato, "Properties of nanocrystalline ZrO$_2$-Y$_2$O$_3$-CeO$_2$-CoO-Al$_2$O$_3$ powders", *Inorg. Mater.*, **47** [10] (2011) 1107–1110.

8. A.G. Belous, E.V. Pashkova, A.N. Makarenko, B.S. Homenko, I.Y. Pyshay, "Effect of synthesis conditions on the formation of yttria-stabilized zirconia", *Inorg. Mater.*, **33** [12] (1997) 1469–1474.

9. V.Ya. Shevchenko, V.B. Glushkova, T.I. Panova, L.I. Podzorova, A.A. Il'icheva, A.E. Lapshin, "Producing ultrafine powders of a tetragonal solid solution in the ZrO$_2$-CeO$_2$ system", *Inorg. Mater.*, **37** [7] (2001) 692–697.

10. L.I. Podzovora, A.A. Il'icheva, N.A. Mikhailina, V.Ya. Shevchenko, L.I. Shvorneva, "Phase formation in the ZrO$_2$-Al$_2$O$_3$-CeO$_2$ system", *Inorg. Mater.*, **38** [12] (2002) 1235–1240.

11. Y. Chen, W. Liu, "Preparation and tribological properties of sol-gel zirconia thin films stabilized with ceria", *J. Mater. Lett.*, **55** [6] (2003) 407–413.

12. O. Vasylkiv, Y. Sakka, "Nonisothermal synthesis of yttria-stabilized zirconia nanopowder through oxalate processing: I. Characteristics of Y-Zr oxalate synthesis and its decomposition", *J. Am. Ceram. Soc.*, **83** [9] (2000) 2196–2202.

13. S. Somiya, R. Roy, "Hydrothermal synthesis of fine oxide powders", *Bull. Mater. Sci.*, **23** [6] (2000) 453–460.

14. E.V. Dudnik, "Modern methods for hydrothermal synthesis of ZrO$_2$-based nanocrystalline powders", *Powder Metall. Metal Ceram.*, **48** [3-4] (2009) 238–248

15. A.V. Shevchenko, E.V. Dudnik, A.K. Ruban, V.P. Red'ko, V.M. Vereschaka, L.M. Lopato, "Nanocrystalline powders based on ZrO$_2$ for materials of biomedical applications and power engineering", *Powder Metall. Metal Ceram.*, **41** [11-12] (2002) 558–563.

16. P.D. Dankov, Reports of the Academy of Sciences, The USSR, **23** (1939) 548.

17. O.V. Al'myasheva, E.N. Korytkova, A.V. Maslov, V.V. Gusarov, "Preparation of nanocrystalline alumina under hydrothermal conditions", *Inorg. Mater.*, **41** [5] (2005) 460–467.

18. E.V. Dudnik, A.K. Shevchenko, A.K. Ruban, V.P. Red'ko, L.M. Lopato, "Synthesis and properties of nanocrystalline 90 wt% ZrO$_2$(Y$_2$O$_3$,CeO$_2$)-10 wt % Al$_2$O$_3$ powder", *Inorg. Mater.*, **44** [4] (2008) 409–413.

19. E.V. Dudnik, A.V. Shevchenko, A.K. Ruban, Z.A. Zaitseva, L.M. Lopato, "Effect of heat treatment on the properties of nanocrystalline 80 wt% Al$_2$O$_3$-20 wt% ZrO$_2$ (CeO$_2$, Y$_2$O$_3$) powder", *Inorg. Mater.*, **44** [5] (2008) 510–514.

20. F. Yu, J. Yang, J. Mab, J. Du, Y. Zhou, "Preparation of nanosized CoAl$_2$O$_4$ powders by sol-gel and sol-gel-Hydrothermal Methods", *J. Alloys Compd.*, **468** [1-2] (2009) 443–446.

21. S. Cava, S.M. Tebcherani, S.A. Pianaro, C.A. Paskocimas, E. Longo, J.A. Varela, "Structural and spectroscopic analysis of γ-Al$_2$O$_3$ to α-Al$_2$O$_3$-CoAl$_2$O$_4$ phase transition", *Mater. Chem. Phys.*, **97** (2006) 102–108.

22. E.V. Dudnik, A.K. Shevchenko, A.K. Ruban, V.P. Red'ko, L.M. Lopato, "Effect of Al$_2$O$_3$ on the properties of nanocrystalline ZrO$_2$ + 3 mol % Y$_2$O$_3$ powder", *Inorg. Mater.*, **46** [2] (2010) 172–176.